IEEE Access
Multidisciplinary | Rapid Review | Open Access Journal

Received 20 May 2024, accepted 28 June 2024, date of publication 2 July 2024, date of current version 12 July 2024.

Digital Object Identifier 10.1109/ACCESS.2024.3421930

RESEARCH ARTICLE

Multi-Objective Dispatch for Batteries and Renewable Generation Sources in Distribution Grids Using a Weighting-Based Convex Approach While Considering Uncertainty

OSCAR DANILO MONTOYA[1], (Senior Member, IEEE), FEDERICO MARTIN SERRA[2], WALTER GIL-GONZÁLEZ[3], (Senior Member, IEEE), LUIS FERNANDO GRISALES-NOREÑA[4], (Member, IEEE), AND JESÚS C. HERNÁNDEZ[5], (Senior Member, IEEE)

[1]Facultad de Ingeniería, Universidad Distrital Francisco José de Caldas, Bogotá 110231, Colombia
[2]Laboratorio de Control Automático (LCA), Facultad de Ingeniería y Ciencias Agropecuarias (FICA), Universidad Nacional de San Luis (UNSL), CONICET, Villa Mercedes, San Luis 5730, Argentina
[3]Department of Electrical Engineering, Universidad Tecnológica de Pereira, Pereira 660003, Colombia
[4]Department of Electrical Engineering, Universidad de Talca, Curico 3340000, Chile
[5]Department of Electrical Engineering, University of Jaén, 23071 Jaén, Spain

Corresponding authors: Oscar Danilo Montoya (odmontoyag@udistrital.edu.co), Jesús C. Hernández (jcasa@ujaen.es), and Luis Fernando Grisales-Noreña (luis.grisales@utalca.cl)

This work was supported in part by the Council of Andalucía (Junta de Andalucía, Consejería de Transformación Económica, Industria, Conocimiento y Universidades, Secretaría General de Universidades, Investigación y Tecnología) under Project ProyExcel-00381; and in part by the Thematic Network "Red para la Integración a Gran Escala de Energías Renovables en Sistemas Eléctricos [RIBIERSE-Ibero-American Program of Science and Technology for Development (CYTED)]" through the Call for Thematic Networks of the CYTED (Ibero-American Program of Science and Technology for Development), in 2022, under Grant 723RT0150.

ABSTRACT This research presents a multi-objective dispatch (MOD) for energy storage systems (ESS) utilizing batteries and renewable energy resources (RES) in distribution network applications. This proposal employs a convex weighting-based approach. The exact MOD nonlinear programming model, which is non-convex due to the power balance constraint, is approximated using a second-order cone equivalent in order to ensure a global optimum, leveraging the convex properties of the objective functions and the conic equivalent in the complex-variable domain. The MOD, based on the linear combination of the objective functions via the weighting-based method, enables the construction of the optimal Pareto front, as each combination of the weighting factors generates a convex optimization sub-problem. The MOD analysis simultaneously considers the minimization of the expected grid operating costs with regard to energy purchasing at the substation terminals, the reduction of the operating costs associated with the RES and the ESS, and the minimization of the expected daily energy losses. This research makes two contributions: 1) the incorporation of the active and reactive power capabilities of the power electronic converters that interface with the ESS and the RES and 2) a robust analysis via convex optimization to address the uncertainties related to the expected daily generation and demand profiles. Numerical results obtained in the IEEE 33- and 85-bus test system confirm the effectiveness and robustness of the proposed MOD in comparison with the continuous genetic algorithm, the particle swarm optimizer, and the vortex search algorithm. In addition, the best metaheuristic technique was employed for constructing the Pareto front and comparing its performance against the

The associate editor coordinating the review of this manuscript and approving it for publication was Ilaria De Munari.

proposed convex approach for the 33-bus grid. In the case of the 85-bus grid, battery power losses were included to demonstrate the effectiveness of this solution methodology in medium-scale distribution grids.

INDEX TERMS Energy losses minimization, grid operating cost minimization, multi-objective dispatch, second-order conic equivalent, robust convex optimization, variable power factor operation, weighting-based multi-objective methodology.

NOMENCLATURE

ACRONYMS

AC	Alternating current.
DER	Distributed energy resource.
ESS	Energy storage system.
MOD	Multi-objective dispatch.
RES	Renewable energy system.
SoC	State of charge.

PARAMETERS

Δ_t	Time period under analysis during a day of operation (h).
SoC_{ki}	Initial SoC of the battery system connected to node k (%).
$\overline{\text{SoC}}$	Maximum SoC value allowed (%).
$\overline{p_{k,\text{inj}}}$	Maximum active power absorption supported by the battery system connected to node k (W).
$\overline{p_{k,\text{inj}}}$	Maximum active power injection supported by the battery system connected to node k (W).
$\overline{s^{\text{g}}}$	Maximum apparent power allowed by the substation connected to node k (V· A).
$\overline{s_k^{\text{b}}}$	Maximum apparent power allowed by the battery system connected to node k (V· A).
$\overline{s_k^{\text{DER}}}$	Maximum apparent power allowed by the DER connected to node k (V· A).
$\overline{s_k^{\text{g}}}$	Maximum current flowing through the distribution line that connects nodes k and m (A).
$\overline{v}$	Maximum voltage magnitude allowed in the nodes (V).
$\underline{\text{SoC}}$	Minimum SoC value allowed (%).
$\underline{s^{\text{g}}}$	Minimum apparent power allowed by the substation connected to node k (V· A).
$\underline{v}$	Minimum voltage magnitude allowed in the nodes (V).
φ_k	Battery charge/discharge coefficient (%/Wh).
C_{1k}	Energy purchasing costs at the substation connected to node k (USD/kWh).
C_{2k}	Operating costs of the DER connected to node k (USD/kWh).
C_{3k}	Operating costs of the battery system connected to node k (USD/kWh).
C_{OF_1}	Operating costs factor to normalize OF_1 (1/kWh).
C_{OF_2}	Operating costs factor to normalize OF_2 (1/USD).
f_{kt}^{DER}	Power availability factor regarding the DER connected to node k during period t.
v^{nom}	Nominal voltage value at substation s.
y_{km}	Admittance at position km of the nodal admittance matrix (S).

SUBSCRIPTS

k, m	Node.
km	Branch.
s	Substation.
t	Period under analysis.

SETS AND OPERATORS

$(\cdot)^*$	Conjugate of the complex argument.
$\lvert\cdot\rvert$	Absolute value of the complex argument.
$\lVert\cdot\rVert_2$	Euclidean norm of the complex argument.
Ω_N	Set containing all network nodes.
Ω_T	Set containing all time periods under analysis.
Ω_L	Set containing all network branches.
real $(\cdot)$	Real part of the complex argument.

VARIABLES

SoC_{kt}	SoC of the battery system connected to node k during period t (%).
SoC_{kt}^{+}	SoC of the battery system connected to node k during the next period t (%).
h_{kt}	Squared magnitude of the voltage at node k during period t (V^2).
s_{kt}^{DER}	Complex power generated by the DER connected to node k during period t (V· A).
s_{kt}^{g}	Complex power demanded by the load connected to node k during period t (V· A).
s_{kt}^{g}	Complex power generated by the substation connected to node k during period t (V· A).
s_{kt}^{v}	Complex power injected/absorbed by the battery system connected to node k during period t (V· A).
v_{st}	Complex voltage value at substation s during period t (V).
w_{kmt}	Product of the conjugate voltage of node k with the voltage of node m during period t (V^2).
v_{kt}	Complex voltage value at node k during period t (V).

I. INTRODUCTION

Recent advances in renewable energy systems (RES) and efficient energy storage systems (ESS) have sparked a global awareness of the urgent need to reduce the carbon footprint resulting associated with human activities [1], [2]. This includes mitigating the adverse effects of human-induced changes in weather patterns due to the significant emissions of pollutants into the atmosphere, a defining trait of the Anthropocene era [3]. For decades, researchers have studied renewable energy generation from various sources, such as solar, wind, geothermal, tidal, and hydraulic power, while aiming for two main benefits: reducing the energy production costs from fossil sources and mitigating the daily emissions of carbon dioxide caused by human consumption in the transportation and electricity sectors [4]. On the other hand, RES have allowed supplying electricity to remote communities far from central transmission or sub-transmission systems. This, based on the concept of *isolated microgrids* [5], [6]. These electrical networks have typically been powered by diesel generation sources. However, with the advancements in renewable energy technologies, this paradigm is shifting, as microgrids can now be powered by solar and wind sources [7]. Nevertheless, even though RES are promising for energy generation and have applications all around the world, they pose two challenges: the unpredictability of renewable energy resources and their non-controllability. This implies that the effective integration of RES must incorporate ESS to address daily variations in generation and demand, thus ensuring the reliability, continuity, and quality of the energy service for all end-users [8], [9].

For electrical network applications, and considering the importance of ESS, recent advances in this area have focused on developing chemical energy storage devices with high energy density and competitive storage costs [10], [11]. In this context, the ideal complements of RES are lithium-ion batteries [12], [13], a technology that has been influenced by advances in electrical vehicle applications. These advances have made them very attractive for electrical grids, as this technology is now mature and has competitive market costs [14], [15]. In essence, the possibility of improving the quality of the service provided by microgrids or active distribution networks lies in the effective coordination of ESS and RES while considering different operation indices and proposing multi-objective optimization methodologies [16], [17].

The concept of *electrical microgrid* is often misunderstood in the current literature. Some authors refer to them as electrical networks that integrate RES and ESS, but they fail to mention their defining feature: their ability to operate in both grid-connected and isolated modes without affecting the energy service [18]. In this sense, an electrical network that incorporates RES and ESS but lacks the capabilities for isolated operation is denoted as an *active distribution network* [19]. Considering these differences, it is worth mentioning that there are multiple approaches to addressing the efficient integration and operation of ESS and RES, each with different objectives, typically focusing on the improvement of technical, economic, or environmental indices. In the case of technical indices, the most typical objective functions are related to energy losses [20], [21], voltage deviations [22], [23], and voltage stability [24], [25]. Regarding the economic objective functions, focus is often placed on the total generation and operation costs of the grid [26] or the expected annual costs of energy losses [27], among others. As for the environmental objective functions, the minimization of the total carbon dioxide emissions prevails, given its direct connection with the effects of global warming and the worldwide commitment to reducing carbon footprints [28]. Some of these approaches, which employ both single- and multi-objective formulations, are presented below.

The authors of [29] presented an energy management system (EMS) for local energy communities based on photovoltaic (PV) sources and an ESS based on batteries, with the aim of reducing greenhouse gas emissions and energy purchasing costs, as well as for increasing energy self-sufficiency. Numerical simulations considering a real electrical microgrid located in Valencia (Spain) and an annual period with a resolution of one hour demonstrated that, when an effective EMS dispatch is implemented, excellent economic and environmental benefits can be obtained in the case of large-scale microgrids with a high penetration of residential users.

The work by [30] suggested the possibility of using batteries for dynamically compensating active and reactive power in medium-voltage distribution grids by effectively controlling the power electronic converters interfacing the batteries. Numerical results in the IEEE 33- and 69-bus networks demonstrated the effectiveness of this approach in comparison with a unitary power factor operation. The EMS was formulated as a nonlinear programming model, and it was solved using GAMS.

The authors of [26] applied three metaheuristic optimizers to deal with the daily dispatch of batteries in a practical way: the continuous genetic algorithm, the parallel version of the vortex search algorithm, and the particle swarm optimizer. Numerical results demonstrated the effectiveness of these algorithms in two test feeders adapted for urban and rural Colombian networks. However, the authors did not perform a multi-objective analysis, in addition to operating the batteries and the RES with a unitary power factor, considerably reducing the potential for dynamic reactive power control in ancillary services.

In [27], an optimization methodology for locating and sizing renewable ESS and batteries in distribution networks was presented. A simulated annealing algorithm was used to determine the location and size of distributed energy resources (DERs), while their operation was defined via a piece-wise linearization technique. Numerical comparisons with conic models demonstrated the effectiveness of this

method in terms of processing times. As expected, both convex approaches reached the optimal solution regarding the objective function values (investment and operating cost reductions). In addition, numerical variations were implemented in feeders with sizes between 11 and 230 nodes.

The study by [31] applied a multi-objective optimization methodology to manage batteries in power systems, which considers the concept of *virtual power plant applications*. Numerical validations using actual data from a low-voltage distribution network in Alice Springs (Northern Territory, Australia) evinced an effective coordination of each user's energy consumption priorities as a function of costs and use preferences. To solve the multi-objective problem, the classical multi-objective non-sorted genetic algorithm was used, and the proposed EMS was validated using the DIgSILENT power factory simulation tool.

In [33], a multi-objective optimization approach was proposed, aimed at defining the optimal location and operation of battery energy storage units in electrical distribution networks while considering useful life maximization together with the minimization of economic and environmental objective functions. A multi-objective equilibrium optimization technique was employed to obtain optimal Pareto fronts while ensuring a diversity of solutions, and the IEEE 30- and 69-bus grids were considered to measure the impact of effective battery coordination in terms of the objective functions analyzed.

Additional works that address the effective coordination of ESS and RES in electrical networks via single- or multi-objective analyses include the multi-objective particle swarm optimization approach [33], the weighting-based optimization approach [34], [35], [36], genetic algorithms [37], [38], the antlion optimizer [39], and the epsilon-constraint method [40].

In this literature review, two major trends can be identified. The first involves the use of metaheuristic optimization algorithms to deal with the location and daily operation of batteries while considering technical, economic, or environmental objective functions with both single- and multi-objective approaches. The second trend examines the possibility of using batteries as dynamic reactive power compensators for increased technical or economic benefits. However, in both contexts, the most common optimization model is an EMS formulated as a nonlinear programming problem, which makes finding the global optimum a difficult task. In light of the above, the following are the main contributions of this research.

i. The efficient EM design problem for RES and ESS in distribution networks undergoes a significant transformation. Originally nonlinear and non-convex, it is converted into a convex approximation via a second-order conic equivalent (SOCE), with the main advantage that the efficiency of the power converters can be considered in the optimization model.
ii. A Pareto front is generated using the weighting-based optimization method to minimize the expected daily energy grid operation costs and energy losses. This is achieved by considering the active and reactive power control capabilities of the power electronic converters interfacing the RES and ESS. In addition, comparisons are made against metaheuristic-based approaches for single- and multi-objective formulations that consider a unitary power factor operation in the RES and ESS.
iii. The stochastic nature of PV generation and daily demand profiles is incorporated via robust optimization, thus maintaining the global optimization capabilities of the SOCE model for the proposed EMS in the context of a multi-objective operation.

Considering the scope of this contribution, it is essential to highlight the following. (i) The location and size of the RES and ESS were provided by the distribution company, which implies that the main interest of this research is to manage these resources efficiently without determining these aspects. (ii) The average PV generation curves and the daily demand profiles were also provided by the distribution company based on historical data on the distribution grid's area of influence, so the robust analysis was performed by adding percent variations of these data. (iii) For the sake of comparison, the benchmark case corresponding to the deterministic scenario considers a unitary factor operation of the RES and ESS. However, additional results are provided which consider a variable power factor, in order to showcase the well-known advantages of dynamic reactive power compensation in active distribution networks. (iv) The evaluation of the proposed SOCE approach in an 85-bus feeder including four PV generation sources and three ESS aims to confirm the effectiveness and robustness of the proposed convex approximation with regard to the numerical improvements reported for the IEEE 33-bus grid system.

As for the first contribution of this research, it is essential to mention that, in the specialized literature, different conic approaches for reformulating power flow problems have been proposed [41], [42]. For example, the authors of [43] applied the branch optimal power flow formulation for managing active and reactive power in distribution networks, aiming to minimize power losses. The branch optimal power flow formulation is a well-known convex approximation for solving the power flow equations in strictly radial distribution networks. However, the effectiveness of its application is conditioned by the use of power losses in the objective function, providing a deteriorated performance for different objective functions. Additionally, the authors of [44] presented a conic approach based on the bus injection reformulation, which can be applied to both radial and meshed distribution networks. Nevertheless, several approximations are required, including trigonometric function transformations. When comparing these approaches to our proposed SOCE, the main advantages of our proposal become evident: its applicability to radial and meshed distribution networks, the possibility of handling different objective functions, and the complex-variable domain reformulation, which is

simpler in comparison with the real-variable analysis reported in [43] and [44].

The remainder of this contribution is structured as follows. Section II describes the general formulation of the multi-objective dispatch problem using a complex-domain variable model aimed at simultaneously minimizing the expected energy losses and the energy purchasing and operating costs of RES and ESS in distribution networks. Section III presents the robust analysis employed to deal with the uncertainties in demand behavior and renewable energy availability. This analysis was performed using the *min/max* concept applicable to convex optimization models, as is the case of the second-order cone programming equivalent used for reformulating the nonlinear programming model that represents the multi-objective dispatch problem. Section IV outlines the main characteristics of the IEEE 33-bus grid, which was adapted to the daily coordination of RES and ESS, considering the actual operating characteristics of a Colombian electrical network with regard to demand profiles, solar generation availability, and daily price variations. Section V lists the main numerical results obtained with the single- and multi-objective approaches, in addition to providing a comparative analysis against metaheuristic optimizers in the literature. In addition, the Pareto fronts are presented, which include uncertainties and allow observing fundamental changes in the objective functions, with variations in renewable energy or demand curves. Finally, Section VI presents the main concluding remarks of this work, as well as some proposals for future research.

II. MULTI-OBJECTIVE DISPATCH MODELING

The proposed multi-objective dispatch (MOD) model for ESS and RES considers two objective functions and their corresponding constraints. These constraints are the nodal potential balance, the power flowing through the distribution lines, the batteries' state of charge (SoC), and the regulation and operation limits of the systems connected to the distribution network.

A. OBJECTIVE FUNCTIONS

The objective function of the MOD model harmonizes two objectives through a weighted formulation [45]. It is aimed at minimizing both the energy losses (OF_1) and the operating costs (OF_2) for a day of operation [46]. This is expressed as follows:

$$\min \mathrm{OF} = \omega \frac{\mathrm{OF}_1}{C_{\mathrm{OF}_1}} + (1-\omega)\frac{\mathrm{OF}_2}{C_{\mathrm{OF}_2}} \tag{1}$$

where $\omega \in [0,1]$ is the weighting factor and C_{OF_1}, and C_{OF_2} are factors that normalize the objective functions OF_1 and OF_2, respectively. These objective functions can be minimized [47]:

$$\mathrm{OF}_1 = \mathrm{real}\left(\sum_{k\in\Omega_T}\sum_{k\in\Omega_N}\sum_{k\in\Omega_N} y_{km} v_{kt} v_{mt}^{*}\right), \tag{2}$$

$$\mathrm{OF}_2 = \sum_{k\in\Omega_N}\sum_{t\in\Omega_T}\mathrm{real}\left(C_{1k}s_{kt}^{\mathrm{g}} + C_{2k}s_{k}^{\mathrm{DER}}\right)\Delta_t + \sum_{k\in\Omega_N}\sum_{t\in\Omega_T} C_{3k}\left|\mathrm{real}\left(s_{kt}^{\mathrm{b}}\right)\right|\Delta_t, \tag{3}$$

where v_{kt} denotes the complex voltage at node k during period t; y_{km} is the admittance at position km of the nodal admittance matrix; s_{kt}^{g} is the complex power generated by the substation connected to node k during period t; s_{kt}^{DER} is the complex power generated by the DER connected to node k during period t; s_{kt}^{b} is the complex power injected/absorbed by the battery connected to node k during period t; C_{1k} represents the energy purchasing costs at the substation connected to node k; C_{2k} and C_{3k} correspond to the operating costs of the DER and the battery system connected to node k, respectively (these costs include daily management, upkeep, and operation); Ω_N and Ω_T are the sets of all nodes and all periods under analysis, respectively; Δ_t represents the time period under analysis within a day of operation; and the operators real $(\cdot)$, $(\cdot)^*$, and $|\cdot|$ denote the real part, the conjugate, and the absolute value of the complex argument, respectively.

B. SET OF CONSTRAINTS FOR THE MOD MODEL

The optimal MOD of RES and ESS requires observing a wide range of constraints based on technical and regulatory considerations. These constraints include factors such as energy balance and operating limits, as well as strict compliance with regulatory requirements. These constraints are explained below:

1) ELECTRICAL SYSTEM CONSTRAINTS

The constraints of the electrical distribution system are determined by the nodal current balance in each node, the minimum and maximum voltage limits established by the applicable regulations, the maximum current flows supported by the distribution lines, and the minimum and maximum power generated by the substation [47].

a: NODAL CURRENT BALANCE

$$\left(\frac{s_{kt}^{\mathrm{g}} + s_{kt}^{\mathrm{DER}} + s_{kt}^{\mathrm{b}} - d_{kt}}{v_{kt}}\right)^{*} = \sum_{k\in\Omega_T}\sum_{m\in\Omega_N} y_{km} v_{mt}, \tag{4}$$

where d_{kt} is the complex power demand at node k during period t.

b: OPERATING VOLTAGE LIMITS

$$v_{st} = v^{\mathrm{nom}} + 0j, \tag{5}$$

$$\overline{v} \geq \|v_{kt}\|_2 \geq \underline{v}, \ \{\forall\, t \in \Omega_T, \ \forall\, k \in \Omega_N\} \tag{6}$$

where v_{st} denotes the voltage values at the substation during period t, and v^{nom} is their nominal value [26].

c: CURRENT FLOW LIMITS

$$\overline{i_{km}} \geq \|y_{km}\,(v_{kt} - v_{mt})\|_2\,\{\forall\, km \in \Omega_L,\ \forall\, t \in \Omega_T\}, \quad (7)$$

where $\overline{i_{km}}$ is the maximum magnitude of the current that can flow through the distribution line connected between nodes k and m, and Ω_L denotes the set that contains all branches in the electrical system [48].

d: SUBSTATION LIMITS

$$\overline{s_k^{\text{g}}} \geq \left\|s_{kt}^{\text{g}}\right\|_2,\ \{\forall\, t \in \Omega_T,\ \forall\, k \in \Omega_N\} \quad (8)$$

$$\overline{s_k^{\text{g}}} \geq \text{real}\left(s_{kt}^{\text{g}}\right) \geq \underline{s_k^{\text{g}}},\ \{\forall\, t \in \Omega_T,\ \forall\, k \in \Omega_N\} \quad (9)$$

where $\overline{s^{\text{g}}}$ and $\underline{s^{\text{g}}}$ denote the maximum and minimum apparent power allowed by the substation connected to node k.

It is important to mention that equality constraint (4) corresponds to the nodal balance of the complex nodal current in each node of the electrical distribution system. This constraint is non-convex since there is an inverse rational term represented by $(v_{kt})^*$. Equality constraint (5) defines the voltage values at the substation, which is better known as the *slack node*. Box constraint (6) plays a crucial role in ensuring compliance with regulatory frameworks. These frameworks define the minimum and maximum voltage values necessary for the optimal functioning of the system. Box constraint (7) ensures that the maximum current limits of the transmission lines are not exceeded. This constraint is also known as a *second-order cone* constraint. The second-order cone constraint (8) limits the maximum apparent power of the substation, while box constraint (9) ensures that its active power remains within the capacity limits.

2) DER CONSTRAINTS

The constraints of the DERs are given by the minimum and maximum apparent power generated, as well as by the maximum active power injected into an electrical system.

a: OPERATING DER LIMITS

$$\overline{s_k^{\text{DER}}} \geq \left\|s_{kt}^{\text{DER}}\right\|_2,\ \{\forall\, t \in \Omega_T,\ \forall\, k \in \Omega_N\} \quad (10)$$

$$\overline{s_k^{\text{DER}}} f_{kt}^{\text{DER}} \geq \text{real}\left(s_{kt}^{\text{DER}}\right) \geq 0,\ \left\{\begin{matrix}\forall\, t \in \Omega_T,\\ \forall\, k \in \Omega_N\end{matrix}\right\} \quad (11)$$

where $\overline{s_k^{\text{DER}}}$ is the maximum apparent power that a DER can inject into or absorb from the electrical system at node k, and $f_{kt}^{\text{DER}} \in [0, 1]$ is a factor corresponding to the energy available from the DER connected to node k during period t. This factor is taken with respect to the maximum apparent power.

Note that the second-order cone constraints (10) and (11) ensure that the apparent and active power of the DER remain within their corresponding limits.

3) BATTERY SYSTEM CONSTRAINTS

The constraints corresponding to the battery systems are determined by the maximum apparent and active power injected into or absorbed by the electrical system, as well as to their SoC.

a: MAXIMUM ACTIVE POWER INJECTION AND ABSORPTION

$$\overline{p_{k,\text{inj}}} \geq \text{real}\left(s_{kt}^{\text{b}}\right) \geq \overline{p_{k,\text{abs}}},\ \{\forall\, t \in \Omega_T,\ \forall\, k \in \Omega_N\} \quad (12)$$

where $\overline{p_{k,\text{inj}}}$ is the maximum active power that can be injected by the battery system connected to node k, and $\overline{p_{k,\text{abs}}}$ is the maximum active power that can be absorbed by it.

b: BATTERY SOC

$$\text{SoC}_{kt}^{+} = \text{SoC}_{kt} - \varphi_k \text{real}\left(s_{kt}^{\text{b}}\right)\Delta_t,\ \left\{\begin{matrix}\forall\, t \in \Omega_T,\\ \forall\, k \in \Omega_N\end{matrix}\right\} \quad (13)$$

$$\text{SoC}_{kt}^{+} = \text{SoC}_{kt_i} - \varphi_k \text{real}\left(s_{kt}^{\text{b}}\right)\Delta_t,\ \left\{\begin{matrix}\forall\, t = t_i,\\ \forall\, k \in \Omega_N\end{matrix}\right\} \quad (14)$$

$$\text{SoC}_{kt} = \text{SoC}_{kf},\ \left\{\forall\, t = t_f,\ \forall\, k \in \Omega_N\right\} \quad (15)$$

$$\overline{\text{SoC}} \geq \text{SoC}_{kt} \geq \underline{\text{SoC}},\ \left\{\forall\, t \in \Omega_T, \forall\, k \in \Omega_N\right\} \quad (16)$$

where SoC_{kt} is the SoC of the battery system connected to node k during period t, while SoC_{kt}^{+} is its SoC in the next period under analysis; φ_k is the charge/discharge coefficient of the battery connected to node k; SoC_{ki} and SoC_{kf} denote the initial and final SoC of the battery system connected to node k, and $\overline{\text{SoC}}$ and $\underline{\text{SoC}}$ determine the maximum and minimum SoC of battery systems.

c: MAXIMUM APPARENT POWER INJECTION AND ABSORPTION

$$\overline{s_k^{\text{b}}} \geq \left\|s_{kt}^{\text{b}}\right\|_2,\ \{\forall\, t \in \Omega_T,\ \forall\, k \in \Omega_N\} \quad (17)$$

where $\overline{s_k^{\text{b}}}$ is the maximum apparent power flow that supports the battery system connected to node k.

Box constraint (12) ensures that the maximum limits regarding active power injection and absorption by the battery systems remain within their capabilities. The equality constraint (13) calculates the SoC of the battery system in the next period, while the equality constraints (14) and (15) establish the initial and final values of the battery systems' SoC. Box constraint (16) ensures that the SoC of the batteries is within their maximum and minimum allowed limits. Finally, the SoC constraint (17) ensures that the ESS apparent power injection and absorption remain within their maximum limits.

III. ROBUST SOCP MODEL

A. SECOND-ORDER CONE APPROXIMATION OF MOD MODEL

Second-order cone approximation has proven to be an excellent method for solving the optimal power flow problem in electrical distribution systems [42]. This section mainly

focuses on specifying (4) [47]. First, this constraint is rewritten as follows:

$$\left(s_{kt}^{\mathrm{g}}+s_{kt}^{\mathrm{DER}}+s_{kt}^{\mathrm{b}}-d_{kt}\right)^{*}=\sum_{k\in\Omega_T}\sum_{m\in\Omega_N}y_{km}w_{kmt}, \tag{18}$$

where w_{kmt} is a complex auxiliary variable defined as

$$w_{kmt}=v_{kt}^{*}v_{mt}.\ \{\forall\, t\in\Omega_T,\ \forall\, k\in\Omega_N\} \tag{19}$$

Note that the constraint (18) is an affine equation, so it is now convex. The issue lies in the complex auxiliary variable defined in (19), which generates a quadratic non-convex constraint [49]. Multiplying by the conjugate of w_{kmt} in (19) yields

$$\begin{aligned} w_{kmt}(w_{kmt})^{*}&=v_{kt}^{*}v_{mt}\left(v_{kt}^{*}v_{mt}\right)^{*}\\ \|w_{kmt}\|_2^2&=\|v_{kt}\|_2^2\,\|v_{mt}\|_2^2\\ \|w_{kmt}\|_2^2&=h_{kt}h_{mt}, \end{aligned} \tag{20}$$

where h_{kt} is a real auxiliary variable set as $h_{kt}=\|v_{kt}\|_2^2$. This constraint can be rewritten as follows:

$$\begin{aligned} \|w_{kmt}\|_2^2&=\frac{1}{4}\left(h_{kt}+h_{mt}\right)^2-\frac{1}{4}\left(h_{kt}-h_{mt}\right)^2\\ 4\,\|w_{kmt}\|_2^2+\left(h_{kt}-h_{mt}\right)^2&=\left(h_{kt}+h_{mt}\right)^2\\ \left\|\begin{pmatrix}2w_{kmt}\\ h_{kt}-h_{mt}\end{pmatrix}\right\|_2&=h_{kt}+h_{mt}. \end{aligned} \tag{21}$$

Note that the hyperbolic constraint (21) remains non-convex [50]. Hence, the equal is relaxed to transform it into a second-order cone constraint:

$$\left\|\begin{pmatrix}2w_{kmt}\\ h_{kt}-h_{mt}\end{pmatrix}\right\|_2\leq h_{kt}+h_{mt}. \tag{22}$$

On the other hand, it is important to mention another constraint that needs to be included for ensuring a logical result from the product between the conjugate voltage of node k and the voltage of node m, as given by (19). This constraint is

$$w_{kmt}=w_{mkt}^{*}.\ \{\forall\, t\in\Omega_T,\ \forall\, km\in\Omega_L\} \tag{23}$$

Constraint (7) is related to the current flow limits of each distribution line and must be expressed as a function of real and complex auxiliary variables [50]. Therefore, this constraint is multiplied by the conjugate of v_{kt}, thus yielding

$$\overline{s_{km}}\geq\left\|y_{km}\left(h_{kt}-w_{kmt}\right)\right\|_2,\ \begin{Bmatrix}\forall\, t\in\Omega_T,\\ \forall\, km\in\Omega_L\end{Bmatrix} \tag{24}$$

where $\overline{s_{km}}$ is the maximum apparent power that can flow through the distribution line that connects nodes k and m.

For ease of reading, the convex version of the entire MOD optimization model is shown below.

a: MOD MODEL OBJECTIVE FUNCTION

$$\begin{aligned} &\min\ \mathrm{OF}\\ &=\omega\frac{\mathrm{OF}_1}{C_{\mathrm{OF}_1}}+(1-\omega)\frac{\mathrm{OF}_2}{C_{\mathrm{OF}_2}} && (25)\\ &\mathrm{OF}_1=\mathrm{real}\left(\sum_{k\in\Omega_T}\sum_{km\in\Omega_L}y_{km}w_{kmt}^{*}\right), && (26)\\ &\mathrm{OF}_2=\sum_{k\in\Omega_N}\sum_{t\in\Omega_T}\mathrm{real}\left(C_{1k}s_{kt}^{\mathrm{g}}+C_{2k}s_{k}^{\mathrm{DER}}\right)\Delta_t\\ &\quad+\sum_{k\in\Omega_N}\sum_{t\in\Omega_T}C_{3k}\left|\mathrm{real}\left(s_{kt}^{\mathrm{b}}\right)\right|\Delta_t, && (27) \end{aligned}$$

b: SET OF CONSTRAINTS

$$\begin{aligned} &\left(s_{kt}^{\mathrm{g}}+s_{kt}^{\mathrm{DER}}+s_{kt}^{\mathrm{b}}-d_{kt}\right)^{*}\\ &\quad=\sum_{k\in\Omega_T}\sum_{m\in\Omega_N}y_{km}w_{kmt}, && (28)\\ &h_{st}=\left(v^{\mathrm{nom}}\right)^2,\ \{\forall\, t\in\Omega_T,\ \forall\, s\in\Omega_N\} && (29)\\ &\overline{v}^2\geq h_{kt}\geq\underline{v}^2,\ \{\forall\, t\in\Omega_T,\ \forall\, k\in\Omega_N\} && (30)\\ &\overline{s_{km}}\geq\left\|y_{km}\left(h_{kt}-w_{kmt}\right)\right\|_2,\ \begin{Bmatrix}\forall\, t\in\Omega_T,\\ \forall\, km\in\Omega_L\end{Bmatrix} && (31)\\ &\overline{s_k^{\mathrm{g}}}\geq\left\|s_{kt}^{\mathrm{g}}\right\|_2,\ \{\forall\, t\in\Omega_T,\ \forall\, k\in\Omega_N\} && (32)\\ &\overline{s_k^{\mathrm{g}}}\geq\mathrm{real}\left(s_{kt}^{\mathrm{g}}\right)\geq\underline{s_k^{\mathrm{g}}},\ \{\forall\, t\in\Omega_T,\ \forall\, k\in\Omega_N\} && (33)\\ &\overline{s_k^{\mathrm{DER}}}\geq\left\|s_{kt}^{\mathrm{DER}}\right\|_2,\ \{\forall\, t\in\Omega_T,\ \forall\, k\in\Omega_N\} && (34)\\ &\overline{s_k^{\mathrm{DER}}f_{kt}^{\mathrm{DER}}}\geq\mathrm{real}\left(s_{kt}^{\mathrm{DER}}\right)\geq 0,\ \begin{Bmatrix}\forall\, t\in\Omega_T,\\ \forall\, k\in\Omega_N\end{Bmatrix} && (35)\\ &\overline{p_{k,\mathrm{inj}}}\geq\mathrm{real}\left(s_{kt}^{\mathrm{b}}\right)\geq\overline{p_{k,\mathrm{abs}}},\ \{\forall\, t\in\Omega_T,\ \forall\, k\in\Omega_N\} && (36)\\ &\mathrm{SoC}_{kt}^{+}=\mathrm{SoC}_{kt}-\varphi_k\mathrm{real}\left(s_{kt}^{\mathrm{b}}\right)\Delta_t,\ \begin{Bmatrix}\forall\, t\in\Omega_T,\\ \forall\, k\in\Omega_N\end{Bmatrix} && (37)\\ &\mathrm{SoC}_{kt}^{+}=\mathrm{SoC}_{kt_i}-\varphi_k\mathrm{real}\left(s_{kt}^{\mathrm{b}}\right)\Delta_t,\ \begin{Bmatrix}\forall\, t=t_i,\\ \forall\, k\in\Omega_N\end{Bmatrix} && (38)\\ &\mathrm{SoC}_{kt}=\mathrm{SoC}_{kf},\ \{\forall\, t=t_f,\ \forall\, k\in\Omega_N\} && (39)\\ &\overline{\mathrm{SoC}}\geq\mathrm{SoC}_{kt}\geq\underline{\mathrm{SoC}},\ \{\forall\, t\in\Omega_T,\forall\, k\in\Omega_N\} && (40)\\ &\overline{s_k^{\mathrm{b}}}\geq\left\|s_{kt}^{\mathrm{b}}\right\|_2,\ \{\forall\, t\in\Omega_T,\ \forall\, k\in\Omega_N\} && (41)\\ &\left\|\begin{pmatrix}2w_{kmt}\\ h_{kt}-h_{mt}\end{pmatrix}\right\|_2\\ &\quad\leq h_{kt}+h_{mt},\ \begin{Bmatrix}\forall\, t\in\Omega_T,\\ \forall\, k,m\in\Omega_N\end{Bmatrix} && (42)\\ &w_{kmt}=w_{mkt}^{*}.\ \{\forall\, t\in\Omega_T,\ \forall\, km\in\Omega_L\} && (43) \end{aligned}$$

Note that this model is convex, so its global optimum can be ensured.

B. INCORPORATING UNCERTAINTY INTO THE MOD MODEL

The dynamic nature of demand and the variable characteristics of primary DERs pose challenges for the operation

of electrical distribution systems. The inherent uncertainties associated with these factors require sophisticated optimization approaches, including stochastic programming [51], [52], [53], chance-constrained optimization [54], and robust optimization [55], [56]. Stochastic and chance-constrained approaches often necessitate a thorough understanding of the probability distribution function for uncertain parameters, which may not be readily available in real-world scenarios. Conversely, robust optimization stands out because it does not require explicit knowledge of probability distribution functions, offering computational manageability and a practical appeal [57], [58].

To implement robust optimization, it is necessary to create a new set that contains the expected mean values of the demand and the available energy factor, along with their corresponding deviations. The new set of uncertainties (Ω_U) is represented as follows:

$$\Omega_U^t(\bar{\mathbf{u}}_t, \hat{\mathbf{u}}_t) := \left\{ \begin{array}{c} \mathbf{u}_t \in \mathbf{R}^{|\Omega_N|} : u_{kt} = \bar{u}_{kt} + \hat{u}_{kt}\left(\theta_{kt}^{+} - \theta_{kt}^{-}\right), \\ \theta_{kt}^{+} + \theta_{kt}^{-} \leq 1, \ \{\forall\, k \in \Omega_N\} \end{array} \right\}, \quad (44)$$

where θ_{kt}^{+} and θ_{kt}^{-} correspond to binary variables used to incorporate the uncertainties into the MOD model; and $\bar{\mathbf{u}}$ represents the expected mean values of the demand and the available energy factor during period t, while $\hat{\mathbf{u}}_t$ corresponds to their corresponding deviations.

The proposed robust model is solved using a two-stage strategy known as *min/max optimization*, where the first stage minimizes a cost function $f^f(\mathbf{x})$ and the second stage maximizes a cost function $f^s(\mathbf{x}, \mathbf{y}, \mathbf{u})$ that incorporates uncertainties to generate the worst-case scenario. *min/max* optimization can be formulated as follows:

$$\begin{aligned} &\min_{\mathbf{x}} f^f(\mathbf{x}) + \max_{\mathbf{u}\in\Omega_U} \left(f^s(\mathbf{x}, \mathbf{y}, \mathbf{u})\right), \\ &\text{subject to} \quad \mathbf{h}^f(\mathbf{x}) = 0, \\ &\qquad\qquad\ \ \mathbf{g}^f(\mathbf{x}) \leq 0, \\ &\qquad\qquad\ \ \mathbf{h}^s(\mathbf{x}, \mathbf{y}, \mathbf{u}) = 0, \\ &\qquad\qquad\ \ \mathbf{g}^s(\mathbf{x}, \mathbf{y}, \mathbf{u}) \leq 0, \end{aligned} \quad (45)$$

where $\mathbf{x}$ is the vector of the decision variable for the first stage; $f^f(\mathbf{x})$, $\mathbf{h}^f(\mathbf{x})$, and $\mathbf{g}^f(\mathbf{x})$ denote the objective function, the set of equality constraints, and the set of inequality constraints for the first stage, respectively; $f^s(\mathbf{x}, \mathbf{y}, \mathbf{u})$, $\mathbf{h}^s(\mathbf{x}, \mathbf{y}, \mathbf{u})$, and $\mathbf{g}^s(\mathbf{x}, \mathbf{y}, \mathbf{u})$ correspond to the objective function, the set of equality constraints, and the set of inequality constraints for the second stage, respectively; and $\mathbf{y}$ is the vector of decision variables for the second stage.

The proposed robust optimization for the MOD model can be easily solved by dividing it into two stages, as outlined in (45). Initially, the first stage computes the decision variable $\mathbf{x}$ related to MOD scheduling without incorporating uncertainties. Although the line current flows are determined at this point, they do not reflect real values and will be fine-tuned in the next stage, which takes a set of uncertainties into account. In the second stage, the decision variables $\mathbf{y}$ and $\hat{\mathbf{u}}$ are computed, and these values are returned to the first stage, which performs recalculations within the framework of an iterative procedure until the values of the objective functions do not change. For more details on this process, please refer to [59].

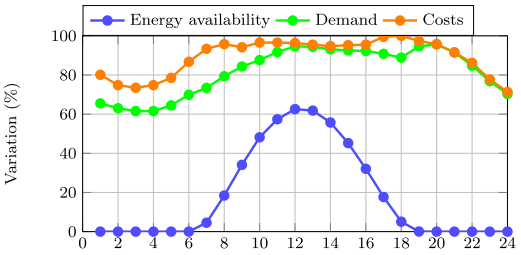

FIGURE 1. Daily generation, demand, and generation costs applicable to the IEEE 33-bus grid in the studied scenario (Medellín, Colombia).

IV. DISTRIBUTION NETWORKS UNDER ANALYSIS

Two test systems were used to validate the proposed MOD model for ESS and RES systems. The first test network corresponds to an adapted version of the IEEE 33-bus grid for the daily expected operational profile of an urban distribution network in Medellín, Colombia. The expected daily demand, PV generation, and hourly slack generation prices for this electrical network are depicted in Figure 1. More details about these curves can be consulted in [26].

The IEEE 33-bus grid is a typical radial distribution network composed of 32 branches and 33 nodes, operating with a line-to-ground voltage of 12660 V at the terminals of bus 1 (*i.e.*, the substation bus). The electrical configuration of this network is presented in Figure 2, where the ESS and the RES are also depicted. Note that the ESS correspond to three batteries located at buses 6, 14, and 31, with nominal energy storage capacities of 2000 kWh, 1000 kWh, and 1500 kWh, respectively. In addition, the ESS connected at bus 6 has charging and discharging times of 5 h, whereas the remaining ESS have 4 h. Furthermore, the PV sources are situated at nodes 13, 25, and 30, with installed capacities of approximately 1125 kW, 1320 kW, and 999 kW, respectively. Finally, the electrical parameters concerning the peak active and reactive power consumption per node, the branch impedance, and the maximum thermal currents can be consulted in [26].

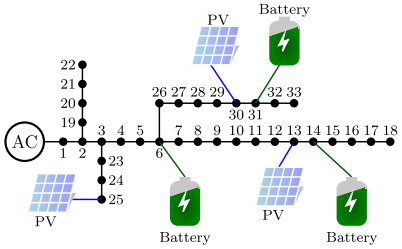

FIGURE 2. Single-line diagram for the first test feeder.

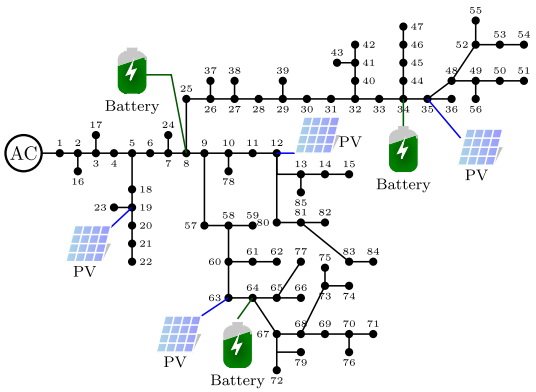

FIGURE 3. Single-line diagram for the second test feeder.

The second test network was also an adapted version of the IEEE 85-bus grid, with the same operation profiles as those used in the first test network (Figure 1). This test system is composed of 84 branches and 85 nodes, and it operates at a rated voltage of 11000 V at the substation bus (bus 1). Furthermore, four RES systems based on PV sources have been included, each with a rated power of 1.5 MW, located at nodes 12, 19, 35, and 63. Three battery-based ESS have been located at buses 8, 34, and 64, with nominal energy storage capacities of 2000 kWh, 1000 kWh, and 1500 kWh, respectively. The charging and discharging times of the batteries are 5 h, 4 h, and 4 h for buses 8, 34, and 64, with installed capacities of approximately 1125 kW, 1320 kW, and 999 kW. Figure 3 depicts the electrical configuration of the second test network, where the ESS and the RES are taken into account.

V. COMPUTATIONAL VALIDATION

All the numerical validations of the proposed MOD approach were conducted using the MATLAB software (version 2023b). These validations were performed with Yalmip (version R20230622), a toolbox for modeling and optimization, and the Gurobi solver (version 10.0.3) [60], [61] on a PC with a 13th Gen Intel(R) Core(TM) i7-13650HX 2.60 GHz processor, 64.0 GB RAM, and a 64-bit version of Microsoft Windows 11 Home.

A. RESULTS FOR THE IEEE 33-BUS NETWORK

To assess the efficacy of the proposed optimization approach in the IEEE 33-bus grid when compared to literature reports, three analyses were conducted. The initial analysis dealt with a single-objective function for operating ESS with unitary and variable power factors. Subsequently, a multi-objective analysis was conducted, also focusing on the unity power factor. The third analysis incorporated variable power factors and addressed uncertainties.

1) SINGLE-OBJECTIVE ANALYSIS

The single-objective analysis considered two possible operating conditions for the RES and the ESS. In the first case, a comparative study with the solutions reported in [26] was carried out, which correspond to metaheuristic optimizers considering a unitary power factor operation. The reported algorithms were the continuous genetic algorithm (CGA), the parallel versions of the particle swarm optimizer (PPSO), and the vortex search algorithm (PVSA). The second simulation case involved the possibility of operating the RES and the EES while considering variable power factors. Note that no uncertainties were included in this simulation.

Table 1 presents this comparative analysis and the unitary and variable power factor solutions reached with the proposed second-order cone equivalent models (SOCEM), which, for the sake of simplicity, are called $SOCEM_1$ and $SOCEM_2$. In Table 1, the base case refers to an operation utilizing maximum power point tracking for the RES while the ESS are out of service.

TABLE 1. Comparative deterministic analysis for the RES and the ESS in the IEEE 33-bus network.

Method	E_{cost} (USD/day)	E_{loss} (kWh/day)
Base case	6999.05300	2484.57466
CGA	6927.84650	2431.47454
PPSO	6905.22318	2380.83359
PVSA	6900.19331	2377.80281
SOCEM_1	6897.69280	2373.40533
SOCEM_2	6766.98979	1266.72210

The numerical results in Table 1 reveal that:

i. SOCEM_1 outperforms the best result in the literature, *i.e.*, the PVSA reported by [26]. The daily expected improvement in the economic objective function value is about 101.3602 dollars per day of operation when the ESS are dispatched, and about 2.5005 dollars per day of operation in contrast with the PVSA's optimal solution (in the case of the daily energy losses; these improvements were 106.7719 and 4.3974kWh/day, respectively). Note that, even though the difference between the PVSA and SOCEM_1 is minimal, the main advantage of the proposed optimization approach is that it always ensures the same numerical results for the same input data, which is not the case for the metaheuristic optimizers, given their stochastic nature.

ii. The CGA and the PPSO got stuck in local optima. However, as previously mentioned, this behavior is expected in metaheuristic optimization, since the analyzed problem involves three ESS. This means that, for a daily period of study, divided into 1 h periods, the number of variables is 72, which is a high dimension to be treated with metaheuristics, especially when they are time-coupled, as observed in Equations (13)–(15).

iii. The addition of variable power factor capabilities to SOCEM_2 shows that, compared to SOCEM_1, additional gains of about 130.7030 dollars per day of operation and 1106.6832 kWh/day can be reached. These results confirm that using the power electronic converters interfacing RES and ESS to inject reactive power into distribution networks helps with energy losses

dynamically, as expected, given their local reactive power compensation properties. In addition, these reactive power injections also reduce the amount of energy required from the terminals of the substation to supply all loads.

To demonstrate the effectiveness of SOCEM$_2$, the exact formulation of the EMS was implemented in the GAMS software, using the large-scale interior point optimizer (IPOPT) [62], and the results were compared against the second-order cone formulation presented by [47] and the semi-definite programming approach in [63]. All these comparisons confirmed that the solutions reported in Table 1 correspond to the global optimum for the single-objective function analysis, *i.e.*, 6766.99 USD and 1266.72 kW.

2) MULTI-OBJECTIVE ANALYSIS WITH UNITARY POWER FACTOR

In this simulation, the best metaheuristic optimizer in Table 1 (PVSA) was selected to construct the Pareto front via the weighting-based optimization approach. The weighting factor ω was set between 0 and 1, using steps of about 0.1. The normalization factors,*i.e.*, C_{OF_1} and C_{OF_2}, were 2, 484.57466 kW and 6, 999.05300 USD, respectively. Figure 4 presents the comparative Pareto front for the proposed convex approach and the PVSA.

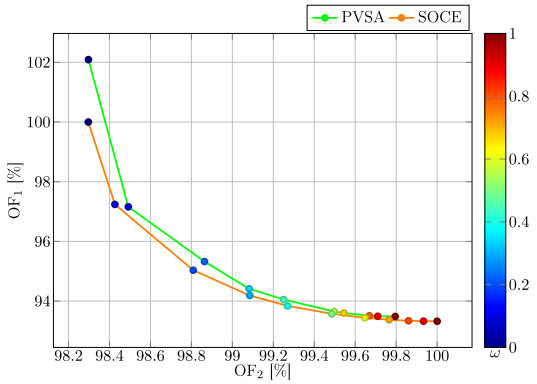

FIGURE 4. Pareto Front comparison for SOCE model and PVSA algorithm. .

The numerical behavior depicted in Figure 4 allows observing that:

i. The proposed SOCEM allows for an improved Pareto front when compared to the PVSA approach, since all the solutions are near the origin of the coordinates. However, both optimization methods can be regarded as adequate. Nevertheless, solution repeatability is only attributable to the proposed convex approximation. The PVSA can converge to a different set of solutions with each execution, given the random nature of metaheuristics.
ii. The extreme solution obtained when the ω factor is set as zero is (2543.24, 6897.56) for the SOCEM, while the PVSA reaches (2596.47, 6897.59), confirming that, in both cases, the optimal solution for minimizing the energy OF$_2$ is obtained by the SOCEM and PVSA. The PVSA improves the numerical solution obtained during the single-objective function analysis (Table 1), but this solution is very similar to the global optimum found with the proposed model.
iii. The extreme solution when the ω factor is set as one is (2373.43, 7017.08) for the SOCEM, while the PVSA approach reaches (2377.52, 7002.70). As expected, these results confirm the SOCEM's ability to ensure the global optimum for OF$_1$, while the PVSA, as reported in Table 1, continues to get stuck in local optima.

It is worth mentioning that the variations in the Pareto front extremes are associated with the multi-modal nature of the MOD, as there are multiple solutions (combination of decision variables) that can provide the same global optimum for one of the objective functions, yielding different results when the other objective function is evaluated.

If a distribution company is interested in selecting one of the solutions from the Pareto front, the 30° and 60° criteria can be applied by generating the area between these angles from the origin of the coordinates. The solutions obtained through this procedure are reported in Table 2.

TABLE 2. Central solutions in the Pareto front using the 30° to 60° criteria.

Method	PVSA	SOCE
Solution #	$(E_{\text{cost}}, E_{\text{loss}})$	$(E_{\text{cost}}, E_{\text{loss}})$
1	(2424.33,6937.36)	(2416.94,6933.51)
2	(2470.97,6911.26)	(2473.05,6906.66)

Note that, for both solution methods, there is a clear compromise: improving one objective function may worsen the other. Nevertheless, regarding OF$_2$, both solutions are better for the SOCE approach, and only in the case of OF$_1$ is the first solution of this model better. The best result for solution 2 is reported by the PVSA. Notwithstanding, with the proposed approach, a better distribution of solutions in the Pareto front can be obtained by reducing the ω-factor steps without compromising the possibility of finding the global optimum. This does not apply to the PVSA, given its metaheuristic nature.

3) MULTI-OBJECTIVE ANALYSIS WITH A VARIABLE POWER FACTOR

Now, in order to validate the MOD in the first test system, two simulation scenarios are considered:

i. $\mathbf{S}_1$: The deterministic MOD, considering a variable power factor operation for the RES and ESS.
ii. $\mathbf{S}_2$: The robust MOD, considering a variable power factor operation for the RES and ESS while including uncertainties in solar generation and demand profiles.

Note that these simulations are only presented for the proposed SOCE approach, as it exhibited better numerical results than the metaheuristic techniques.

Figure 5 depicts the Pareto front of the MOD model, wherein ω is varied between 0 and 1 in steps of 0.01.

It is important to mention that scenario $\mathbf{S}_2$ uses the same normalized coefficients as the deterministic case, *i.e.*, $C_{\mathrm{OF}_1} = 1,478.1476$ kW and $C_{\mathrm{OF}_2} = 6,847.943$ USD.

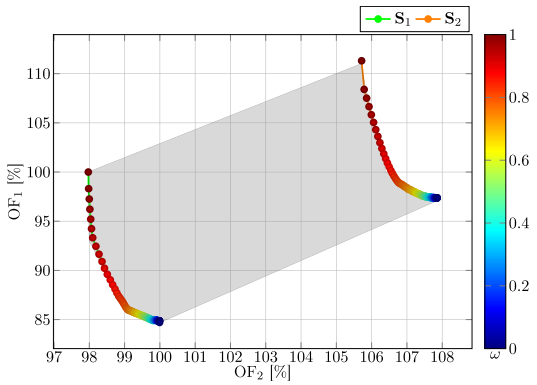

FIGURE 5. Pareto Front for scenarios $\mathbf{S}_1$ and $\mathbf{S}_2$.

Based on Figure 5, it can be concluded that:

i. The incorporation of uncertainty into the MOD model leads to increased objective function values. This highlights the significant influence of demand and DER energy availability. It is crucial to note that robust optimization aims to find a solution that can withstand adverse conditions, ultimately producing a conservative optimal solution. $\mathbf{S}_2$ yields higher objective function values with respect to the deterministic optimization model.
ii. If $\omega = 1$ (see red circle in Figure 5), OF_1 increases by approximately 14.93$ in $\mathbf{S}_2$ when compared to $\mathbf{S}_1$. This increase causes OF_1 to go from 1266.72210 kWh/day to 1455.8437 kWh/day, resulting in additional energy losses of 189.1216 kWh/day. Meanwhile, OF_2 increases by around 7.85% when comparing the robust scenario against the deterministic one. This comparison shows that the daily operating costs increase by USD 537.9742.
iii. For the case where $\omega = 0$ (see blue circle in Figure 5), OF_2 increases by approximately 7.90% in the robust scenario ($\mathbf{S}_2$) when compared to the deterministic one ($\mathbf{S}_1$). This results in an increase from USD 6766.98979 to USD 7301.8364 per day (OF_2), leading to additional daily operating costs of USD 534.8466. At the same time, OF_1 increases by around 11.13% for $\mathbf{S}_2$ with respect to $\mathbf{S}_1$. This modification leads to a daily increase of 164.5178 kWh in the energy losses ($\mathbf{S}_2$).
iv. OF_1 exhibits significant variations in the Pareto front for the deterministic and the robust case (see the blue circles in Figure 5). These variations are 15.29% and 13.94% for $\mathbf{S}_1$ and $\mathbf{S}_2$, respectively.
v. Any solution within the deterministic model and including an uncertainty of 5% or less in the demand and/or available energy of the DER will fall within the gray box. This allows the utility to measure its operating costs or energy losses on a daily basis, thus facilitating decision-making.

B. RESULTS FOR THE IEEE 85-BUS NETWORK

This section evaluates the performance of the robust SOCEM in the second proposed test network. A battery model was used which incorporates the power losses during charging and discharging. In this vein, the set of constraints presented from (36) to (38) must be modified as follows:

$$0 \leq p_{kt,\mathrm{inj}} \leq \overline{p_{k,\mathrm{inj}}} y_{kt}, \tag{46}$$

$$0 \leq p_{kt,\mathrm{abs}} \leq \overline{p_{k,\mathrm{abs}}} z_{kt}, \tag{47}$$

$$\mathrm{SoC}^{+}_{kt} = \mathrm{SoC}_{kt} - \varphi \left(\eta^{a}_{k} p_{k,\mathrm{abs}} - - \frac{1}{\eta^{o}_{k}} p_{k,\mathrm{inj}} \right) \Delta_t, \tag{48}$$

$$\mathrm{SoC}^{+}_{kt} = \mathrm{SoC}_{kt_i} - \varphi \left(\eta^{a}_{k} p_{k,\mathrm{abs}} - \frac{1}{\eta^{o}_{k}} p_{k,\mathrm{inj}} \right) \Delta_t, \tag{49}$$

$$\mathrm{real}\left(s^{\mathrm{b}}_{kt}\right) = p_{k,\mathrm{inj}} - p_{k,\mathrm{abs}}, \tag{50}$$

$$0 \leq y_{kt} \leq 1, \tag{51}$$

$$0 \leq z_{kt} \leq 1, \tag{52}$$

$$y_{kt} + z_{kt} \leq 1, \tag{53}$$

where $p_{kt,\mathrm{inj}}$ and $p_{kt,\mathrm{inj}}$ represent the active power injected and absorbed by the battery system connected at node k during period t; y_{kt} and z_{kt} are auxiliary variables representing the charging and discharging states of the battery system at node k during period t; and $\eta^{a}_{k} = 0.85$ and $\eta^{i}_{k} = 0.9$ correspond to the efficiency rate of the battery system at node k during period t during charging and discharging. For more details on this model, refer to [64].

In order to validate the MOD in the second test system, three simulation cases were considered:

i. $\mathbf{C}_1$: The deterministic MOD, considering a variable power factor operation for the RES and ESS.
ii. $\mathbf{C}_2$: The robust MOD, considering a variable power factor operation for the RES and ESS while including uncertainties in solar generation and demand profiles.
iii. $\mathbf{C}_3$: This case is similar to C2, albeit with the addition of the energy losses of battery systems, as described in (46)–(53).

Figure 5 illustrates the Pareto front for the second test system, wherein ω varies between 0 and 1 in steps of 0.01. It is important to mention that $\mathbf{C}_2$ and $\mathbf{C}_3$ are normalized using the same coefficients of $\mathbf{C}_1$, *i.e.*, $C_{\mathrm{OF}_1} = 1,503.8585$ kW and $C_{\mathrm{OF}_2} = 4,285.6993$ USD.

From Figure 6, it is possible to infer that:

i. Similarly to the results shown in Figure 5, the incorporation of uncertainty into the MOD model results in higher objective function values, emphasizing the impact of demand and DER energy availability. Robust optimization aims to find a solution that can withstand adverse conditions, ultimately leading to a conservative optimal outcome. Furthermore, including the energy losses of the batteries reduces the efficiency of the test system. Therefore, the MOD model produces higher

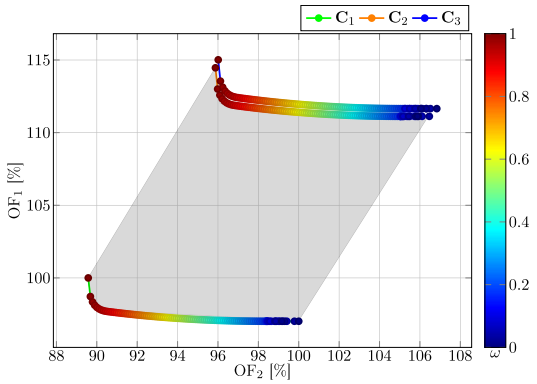

FIGURE 6. Pareto Front for $\mathbf{C_1}$, $\mathbf{C_2}$, and $\mathbf{C_3}$.

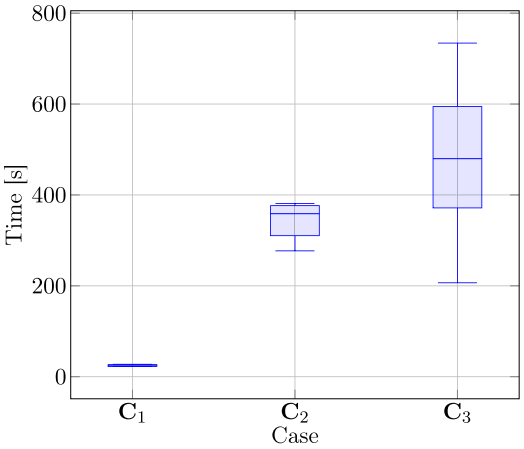

FIGURE 7. Computation time for $\mathbf{C_1}$, $\mathbf{C_2}$, and $\mathbf{C_3}$.

objective function values for $\mathbf{C}_3$ than for $\mathbf{C}_2$, which is a logical result.

ii. For $\omega = 1$ (as indicated by the red circle in Figure 6) in $\mathbf{C}_2$, OF_1 increases by about 14.46%. Thus, the energy losses go from 1503.8585 kWh/day to 1721.3164 kWh/day, *i.e.*, 217.4579 kWh/day when compared to $\mathbf{C}_1$. When the battery energy losses are included, OF_1 increases by approximately 1.0%, indicating that this aspect does not have a significant impact on the daily operation of the test system. As for OF_2, $\mathbf{C}_2$ and $\mathbf{C}_3$ show increases of about 6.30% and 6.44% when compared to $\mathbf{C}_1$, which is equivalent to operating cost increments of USD 431.4204 and USD 441.0075 per day.

iii. For $\omega = 0$ (as indicated by the blue circle in Figure 6), OF_2 increases by approximately 5.88% and 6.84% in $\mathbf{C}_2$ and $\mathbf{C}_3$ when compared to the deterministic case. This results in in a daily operating cost increase of USD 402.6590 and USD 468.3993 per day. At the same time, OF_1 increases by around 14.10% and 14.64% for cases $\mathbf{C}_2$ and $\mathbf{C}_3$. This modification leads to daily increases of 212.0440 kWh and 220.1648 kWh in the energy losses of $\mathbf{C}_2$ and $\mathbf{C}_3$, respectively.

iv. The inclusion of battery energy losses causes no significant change in the Pareto front for $\mathbf{C}_2$ and $\mathbf{C}_3$. These changes are lower than or equal to 1% in both objective functions in both cases, implying no significant effect on the performance of the MOD model.

v. Any solution in $\mathbf{C}_1$ that incorporates an uncertainty of $\pm 5\%$ or less regarding the demand and/or the available energy of the DER will be contained in the gray box in Figure 6. This allows the utility company to monitor its daily operating costs or energy losses, thereby aiding in decision-making.

Finally, Figure 7 illustrates the minimum, maximum, and average computation times for $\mathbf{C}_1$, $\mathbf{C}_2$, and $\mathbf{C}_3$. These times were obtained by running the MOD model 100 times with $\omega = 0.5$. Note that the deterministic case requires the shortest simulation time. This can be attributed to the simplicity of $\mathbf{C}_1$ compared to the others, as it involves fewer variables and does not require solving a min / max problem. Conversely, the simulation times for $\mathbf{C}_2$ and $\mathbf{C}_3$ increase by factors of 13.65 and 19.61. This is due to the increased complexity and computational requirements associated these cases, which involve uncertainties in demand and PV generation.

VI. CONCLUSION

This research addressed the problem regarding the effective coordination of ESS and RES in distribution grids by considering a variable power factor operation through the dynamic active and reactive power control of the power electronic converters interfacing all DERs. In addition, a multi-objective dispatch was considered to simultaneously minimize the expected energy losses and operating costs (*i.e.*, energy purchasing and the operating costs of the RES and the ESS). The main contribution of this research lies in its analysis of uncertainties in the daily dispatch of DERs (*i.e.*, in daily demand profiles and solar generation availability), within the framework of a multi-objective model. A SOCEM was formulated to obtain a robust convex optimization model. The weighting-based optimization approach was implemented to elaborate the optimal Pareto front. The main results are summarized below.

i. A single-objective analysis regarding energy losses and grid operating costs demonstrated that the proposed SOCP formulation surpasses the results obtained with metaheuristic optimization algorithms reported in the literature (*i.e.,* the continuous genetic algorithm and the parallel versions of the vortex search algorithm and the particle swarm optimizer), with the main advantage that, given the convex nature of the SOCP equivalent, an optimal solution is ensured for the same set of input parameters, which is not possible with random optimizers.

ii. Including variable power factor operation capabilities to the DERs improved the expected daily energy losses by about 1106.6832 kWh/day and the expected daily operating costs by about USD 130.7030 when

compared to the unitary power factor operation scenario (for the first test system). These results confirm the effectiveness of dynamic reactive power compensation and its application to distribution networks in order to enhance voltage profiles and reduce energy losses, with the latter being directly linked to the expected reductions in energy purchasing costs.

iii The construction of the Pareto front via the weighting-based optimization approach while considering the deterministic case and inherent uncertainties demonstrated that (a) the deterministic operation scenario provides the lowest admissible objective function values for the energy losses and the operating costs of the grid; (b) the addition of uncertainties in renewable generation and demand provide the highest possible limits for both objective functions; and (c) the expected final daily energy losses and grid operating costs will be contained between the deterministic and robust Pareto fronts, as a function of the accuracy of the distribution company's projection regarding the expected renewable energy availability and power consumption.

Note that the main limitation of this research corresponds to the small sizes of the RES and the ESS, as they limit the potential of coordinating both resources to maximize the distribution company's profits. This limitation was evidenced when the operation of the PV plants was left untouched. The optimal solution showed that these systems continued to operate via maximum power point tracking, which means that the sizes assigned to these RES were not adequately designed to allow storing surplus energy during solar generation peaks, which would be later used at night when the demand increases and the resource is not available.

As future work, the following studies could be conducted: (i) the addition of uncertainties in the expected hourly price of energy while including residential, commercial, and industrial demand curves; (ii) the possibility of reallocating batteries in nodes where additional gains regarding energy losses and daily operating costs can be obtained; and (iii) the extension of the proposed MOD model to direct current distribution networks with monopolar or bipolar operating configurations.

REFERENCES

[1] A. Suman, "Role of renewable energy technologies in climate change adaptation and mitigation: A brief review from Nepal," *Renew. Sustain. Energy Rev.*, vol. 151, Nov. 2021, Art. no. 111524.

[2] R. Li, Q. Wang, and L. Li, "Does renewable energy reduce per capita carbon emissions and per capita ecological footprint? New evidence from 130 countries," *Energy Strategy Rev.*, vol. 49, Sep. 2023, Art. no. 101121.

[3] M. R. Raupach and J. G. Canadell, "Carbon and the anthropocene," *Current Opinion Environ. Sustainability*, vol. 2, no. 4, pp. 210–218, Oct. 2010.

[4] D. Adu, D. Jianguo, R. O. Darko, E. Baffour G., and S. N. Asomani, "Overcoming CO_2 emission from energy generation by renewable hydropower—The role of pump as turbine," *Energy Rep.*, vol. 9, pp. 114–118, Nov. 2023.

[5] A. F. Bastos and R. D. Trevizan, "Feasibility of 100% renewable-energy-powered microgrids serving remote communities," in *Proc. IEEE Power Energy Soc. Innov. Smart Grid Technol. Conf. (ISGT)*, Jan. 2023, pp. 1–5.

[6] E. Semshchikov, M. Negnevitsky, J. Hamilton, and X. Wang, "Cost-efficient strategy for high renewable energy penetration in isolated power systems," *IEEE Trans. Power Syst.*, vol. 35, no. 5, pp. 3719–3728, Sep. 2020.

[7] P. Sokolnikova, P. Lombardi, B. Arendarski, K. Suslov, A. M. Pantaleo, M. Kranhold, and P. Komarnicki, "Net-zero multi-energy systems for Siberian rural communities: A methodology to size thermal and electric storage units," *Renew. Energy*, vol. 155, pp. 979–989, Aug. 2020.

[8] W. Wang, B. Yuan, Q. Sun, and R. Wennersten, "Application of energy storage in integrated energy systems—A solution to fluctuation and uncertainty of renewable energy," *J. Energy Storage*, vol. 52, Aug. 2022, Art. no. 104812.

[9] M. Y. Worku, "Recent advances in energy storage systems for renewable source grid integration: A comprehensive review," *Sustainability*, vol. 14, no. 10, p. 5985, May 2022.

[10] M. R. Chakraborty, S. Dawn, P. K. Saha, J. B. Basu, and T. S. Ustun, "A comparative review on energy storage systems and their application in deregulated systems," *Batteries*, vol. 8, no. 9, p. 124, Sep. 2022.

[11] M. Amir, R. G. Deshmukh, H. M. Khalid, Z. Said, A. Raza, S. M. Muyeen, A.-S. Nizami, R. M. Elavarasan, R. Saidur, and K. Sopian, "Energy storage technologies: An integrated survey of developments, global economical/environmental effects, optimal scheduling model, and sustainable adaption policies," *J. Energy Storage*, vol. 72, Nov. 2023, Art. no. 108694.

[12] A. Lennon, Y. Jiang, C. Hall, D. Lau, N. Song, P. Burr, C. P. Grey, and K. J. Griffith, "High-rate lithium ion energy storage to facilitate increased penetration of photovoltaic systems in electricity grids," *MRS Energy Sustainability*, vol. 6, no. 1, pp. 1–18, Jun. 2019.

[13] H. Shi, M. Liu, Y. Li, S. Wang, C. Qiu, M. Cheng, J. Yuan, K. Yang, and C. Kang, "Multi-objective optimization of integrated lithium-ion battery thermal management system," *Appl. Thermal Eng.*, vol. 223, Mar. 2023, Art. no. 119991.

[14] B. Diouf and C. Avis, "The potential of li-ion batteries in ECOWAS solar home systems," *J. Energy Storage*, vol. 22, pp. 295–301, Apr. 2019.

[15] G. Meng, Y. Sun, T. Yu, C. Wang, K. Sun, and P. An, "A multi-objective control strategy of the energy storage system in distribution networks with a high proportion of renewable energy," *J. Phys., Conf. Ser.*, vol. 2520, no. 1, Jun. 2023, Art. no. 012005.

[16] W. Gil-González, O. D. Montoya, E. Holguín, A. Garces, and L. F. Grisales-Noreña, "Economic dispatch of energy storage systems in DC microgrids employing a semidefinite programming model," *J. Energy Storage*, vol. 21, pp. 1–8, Feb. 2019.

[17] B. Caicedo-Bravo, J. Mora-Flórez, C. Orozco-Henao, H. Salazar-Isaza, and J. Tibaquirá-Giraldo, *Integration of Non-Conventional Renewable Sources of Energy in Developing Countries—Challenges and Opportunities in the Colombian Case*, 1st ed., Pereira, Colombia: Editorial Universidad Tecnológica de Pereira, 2024.

[18] R. Wu and G. Sansavini, "Active distribution networks or microgrids? Optimal design of resilient and flexible distribution grids with energy service provision," *Sustain. Energy, Grids Netw.*, vol. 26, Jun. 2021, Art. no. 100461.

[19] H. Kiani, K. Hesami, A. Azarhooshang, S. Pirouzi, and S. Safaee, "Adaptive robust operation of the active distribution network including renewable and flexible sources," *Sustain. Energy, Grids Netw.*, vol. 26, Jun. 2021, Art. no. 100476.

[20] P. Lazzeroni and M. Repetto, "Optimal planning of battery systems for power losses reduction in distribution grids," *Electr. Power Syst. Res.*, vol. 167, pp. 94–112, Feb. 2019.

[21] K. Chellappan, V. S. S. C. S. Murty, N. Krishnan, G. Sharma, and T. Senjyu, "Real power loss minimization considering multiple DGs and battery in distribution system," *Electric Power Compon. Syst.*, vol. 49, nos. 6–7, pp. 563–572, Apr. 2021.

[22] H. M. A. Ahmed, A. S. A. Awad, M. H. Ahmed, and M. M. A. Salama, "Mitigating voltage-sag and voltage-deviation problems in distribution networks using battery energy storage systems," *Electric Power Syst. Res.*, vol. 184, Jul. 2020, Art. no. 106294.

[23] K. Mahmoud and M. Lehtonen, "Three-level control strategy for minimizing voltage deviation and flicker in PV-rich distribution systems," *Int. J. Electr. Power Energy Syst.*, vol. 120, Sep. 2020, Art. no. 105997.

[24] K. Mardanimajd, S. Karimi, and A. Anvari-Moghaddam, "Voltage stability improvement in distribution networks by using soft open points," *Int. J. Electr. Power Energy Syst.*, vol. 155, Jan. 2024, Art. no. 109582.

[25] O. B. Adewuyi, R. Shigenobu, K. Ooya, T. Senjyu, and A. M. Howlader, "Static voltage stability improvement with battery energy storage considering optimal control of active and reactive power injection," *Electric Power Syst. Res.*, vol. 172, pp. 303–312, Jul. 2019.

[26] L. F. Grisales-Noreña, B. Cortés-Caicedo, O. D. Montoya, J. C. Hernandéz, and G. Alcalá, "A battery energy management system to improve the financial, technical, and environmental indicators of Colombian urban and rural networks," *J. Energy Storage*, vol. 65, Aug. 2023, Art. no. 107199.

[27] A. Valencia, R. A. Hincapie, and R. A. Gallego, "Optimal location, selection, and operation of battery energy storage systems and renewable distributed generation in medium–low voltage distribution networks," *J. Energy Storage*, vol. 34, Feb. 2021, Art. no. 102158.

[28] B. Cortés-Caicedo, L. F. Grisales-Noreña, O. D. Montoya, and R. I. Bolaños, "Optimization of BESS placement, technology selection, and operation in microgrids for minimizing energy losses and CO_2 emissions: A hybrid approach," *J. Energy Storage*, vol. 73, Dec. 2023, Art. no. 108975.

[29] Á. Manso-Burgos, D. Ribó-Pérez, T. Gómez-Navarro, and M. Alcázar-Ortega, "Local energy communities modelling and optimisation considering storage, demand configuration and sharing strategies: A case study in Valencia (Spain)," *Energy Rep.*, vol. 8, pp. 10395–10408, Nov. 2022.

[30] O. D. Montoya and W. Gil-González, "Dynamic active and reactive power compensation in distribution networks with batteries: A day-ahead economic dispatch approach," *Comput. Electr. Eng.*, vol. 85, Jul. 2020, Art. no. 106710.

[31] H. Song, M. Gu, C. Liu, A. M. Amani, M. Jalili, L. Meegahapola, X. Yu, and G. Dickeson, "Multi-objective battery energy storage optimization for virtual power plant applications," *Appl. Energy*, vol. 352, Dec. 2023, Art. no. 121860.

[32] A. A. Abou El-Ela, R. A. El-Sehiemy, A. M. Shaheen, W. A. Wahbi, and M. T. Mouwafi, "A multi-objective equilibrium optimization for optimal allocation of batteries in distribution systems with lifetime maximization," *J. Energy Storage*, vol. 55, Nov. 2022, Art. no. 105795.

[33] P. Kayal, "A multi-objective optimization approach to allocate battery and capacitor in distribution network," in *Proc. 12th Int. Conf. Knowl. Smart Technol. (KST)*, Jan. 2020, pp. 52–57.

[34] X. Zhao, Y. Yang, M. Qin, and Q. Xu, "Multi-objective optimization of distribution network considering battery charging and swapping station," *Energy Rep.*, vol. 9, pp. 1282–1290, Oct. 2023.

[35] D. Bammeke, J. D. Nixon, J. Brusey, and E. Gaura, "Multi-objective energy management model for stand-alone photovoltaic-battery systems: Application to refugee camps," in *Energy and Sustainable Futures: Proceedings of the 3rd ICESF, 2022*. Cham, Switzerland: Springer, 2022, pp. 81–91.

[36] F. Molina-Martin, O. D. Montoya, L. F. Grisales-Noreña, J. C. Hernández, and C. A. Ramírez-Vanegas, "Simultaneous minimization of energy losses and greenhouse gas emissions in AC distribution networks using BESS," *Electronics*, vol. 10, no. 9, p. 1002, Apr. 2021.

[37] A. Afzal and M. K. Ramis, "Multi-objective optimization of thermal performance in battery system using genetic and particle swarm algorithm combined with fuzzy logics," *J. Energy Storage*, vol. 32, Dec. 2020, Art. no. 101815.

[38] L. Zhang, L. Wang, G. Hinds, C. Lyu, J. Zheng, and J. Li, "Multi-objective optimization of lithium-ion battery model using genetic algorithm approach," *J. Power Sources*, vol. 270, pp. 367–378, Dec. 2014.

[39] K. Hosseini, S. Araghi, M. B. Ahmadian, and V. Asadian, "Multi-objective optimal scheduling of a micro-grid consisted of renewable energies using multi-objective ant lion optimizer," in *Proc. Smart Grid Conf. (SGC)*, Dec. 2017, pp. 1–8.

[40] N. Hashemipour, J. Aghaei, M. Lotfi, T. Niknam, M. Askarpour, M. Shafie-Khah, and J. P. S. Catalão, "Multi-objective optimisation method for coordinating battery storage systems, photovoltaic inverters and tap changers," *IET Renew. Power Gener.*, vol. 14, no. 3, pp. 475–483, Jan. 2020.

[41] M. Farivar and S. H. Low, "Branch flow model: Relaxations and convexification—Part II," *IEEE Trans. Power Syst.*, vol. 28, no. 3, pp. 2565–2572, Aug. 2013.

[42] Z. Yuan and M. R. Hesamzadeh, "Second-order cone AC optimal power flow: Convex relaxations and feasible solutions," *J. Modern Power Syst. Clean Energy*, vol. 7, no. 2, pp. 268–280, Mar. 2019.

[43] H. Gao, J. Liu, and L. Wang, "Robust coordinated optimization of active and reactive power in active distribution systems," *IEEE Trans. Smart Grid*, vol. 9, no. 5, pp. 4436–4447, Sep. 2018.

[44] R. A. Jabr, R. Singh, and B. C. Pal, "Minimum loss network reconfiguration using mixed-integer convex programming," *IEEE Trans. Power Syst.*, vol. 27, no. 2, pp. 1106–1115, May 2012.

[45] L. Tang, W. Xu, X. Wang, D. Dong, X. Xiao, and Y. Zhang, "Weighting factors optimization of model predictive control based on fuzzy thrust constraints for linear induction machine," *IEEE Trans. Appl. Supercond.*, vol. 31, no. 8, pp. 1–5, Nov. 2021.

[46] V. M. Garrido-Arévalo, O. D. Montoya, W. Gil-González, L. F. Grisales-Noreña, and J. C. Hernández, "An SDP relaxation in the complex domain for the efficient coordination of BESS and DGs in single-phase distribution grids while considering reactive power capabilities," *J. Energy Storage*, vol. 90, Jun. 2024, Art. no. 111913.

[47] V. M. Garrido-Arévalo, W. Gil-González, O. D. Montoya, L. F. Grisales-Noreña, and J. C. Hernández, "Optimal dispatch of DERs and battery-based ESS in distribution grids while considering reactive power capabilities and uncertainties: A second-order cone programming formulation," *IEEE Access*, vol. 12, pp. 48497–48510, 2024.

[48] O. D. Montoya, L. F. Grisales-Noreña, and W. Gil-González, "Multi-objective battery coordination in distribution networks to simultaneously minimize CO_2 emissions and energy losses," *Sustainability*, vol. 16, no. 5, p. 2019, Feb. 2024.

[49] O. D. Montoya, O. D. Florez-Cediel, and W. Gil-González, "Efficient day-ahead scheduling of PV-STATCOMs in medium-voltage distribution networks using a second-order cone relaxation," *Computers*, vol. 12, no. 7, p. 142, Jul. 2023.

[50] A. Garces, *Mathematical Programming for Power Systems Operation With Applications in Python*, 1st ed., Hoboken NJ, USA: Wiley, Nov. 2021.

[51] M. Peker, A. S. Kocaman, and B. Y. Kara, "A two-stage stochastic programming approach for reliability constrained power system expansion planning," *Int. J. Electr. Power Energy Syst.*, vol. 103, pp. 458–469, Dec. 2018.

[52] M. Peker, A. S. Kocaman, and B. Y. Kara, "Benefits of transmission switching and energy storage in power systems with high renewable energy penetration," *Appl. Energy*, vol. 228, pp. 1182–1197, Oct. 2018.

[53] J. Wang, N. Zhou, and Q. Wang, "Data-driven stochastic service restoration in unbalanced active distribution networks with multi-terminal soft open points," *Int. J. Electr. Power Energy Syst.*, vol. 121, Oct. 2020, Art. no. 106069.

[54] D. Huo, C. Gu, D. Greenwood, Z. Wang, P. Zhao, and J. Li, "Chance-constrained optimization for integrated local energy systems operation considering correlated wind generation," *Int. J. Electr. Power Energy Syst.*, vol. 132, Nov. 2021, Art. no. 107153.

[55] H. Ji, C. Wang, P. Li, F. Ding, and J. Wu, "Robust operation of soft open points in active distribution networks with high penetration of photovoltaic integration," *IEEE Trans. Sustain. Energy*, vol. 10, no. 1, pp. 280–289, Jan. 2019.

[56] D. Bertsimas, E. Litvinov, X. A. Sun, J. Zhao, and T. Zheng, "Adaptive robust optimization for the security constrained unit commitment problem," *IEEE Trans. Power Syst.*, vol. 28, no. 1, pp. 52–63, Feb. 2013.

[57] I. Sarantakos, M. Peker, N.-M. Zografou-Barredo, M. Deakin, C. Patsios, T. Sayfutdinov, P. C. Taylor, and D. Greenwood, "A robust mixed-integer convex model for optimal scheduling of integrated energy storage—Soft open point devices," *IEEE Trans. Smart Grid*, vol. 13, no. 5, pp. 4072–4087, Sep. 2022.

[58] A. Gholami, T. Shekari, and S. Grijalva, "Proactive management of microgrids for resiliency enhancement: An adaptive robust approach," *IEEE Trans. Sustain. Energy*, vol. 10, no. 1, pp. 470–480, Jan. 2019.

[59] B. Zeng and L. Zhao, "Solving two-stage robust optimization problems using a column-and-constraint generation method," *Oper. Res. Lett.*, vol. 41, no. 5, pp. 457–461, Sep. 2013.

[60] J. Lofberg, "YALMIP: A toolbox for modeling and optimization in MATLAB," in *Proc. IEEE Int. Conf. Robot. Autom.*, Taiwan, Sep. 2004, pp. 284–289.

[61] Gurobi Optimization. (2023). *Gurobi Optimizer Reference Manual*. [Online]. Available: https://www.gurobi.com

[62] D. S. Guzmán-Romero, B. Cortés-Caicedo, and O. D. Montoya, "Development of a MATLAB-GAMS framework for solving the problem regarding the optimal location and sizing of PV sources in distribution networks," *Resources*, vol. 12, no. 3, p. 35, Mar. 2023.

[63] X. Bai, H. Wei, K. Fujisawa, and Y. Wang, "Semidefinite programming for optimal power flow problems," *Int. J. Electr. Power Energy Syst.*, vol. 30, nos. 6–7, pp. 383–392, Jul. 2008.
[64] D. Pozo, "Linear battery models for power systems analysis," *Electr. Power Syst. Res.*, vol. 212, Nov. 2022, Art. no. 108565.

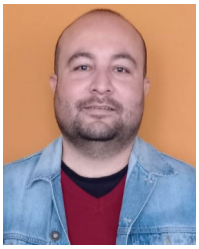

OSCAR DANILO MONTOYA (Senior Member, IEEE) was born in Obando, Valle, Colombia, in 1989. He received the B.E.E., M.Sc., and Ph.D. degrees in electrical engineering from Universidad Tecnológica de Pereira, Colombia, in 2012, 2014, and 2019, respectively. He is currently an Assistant Professor of electrical engineering program with Universidad Distrital Francisco José de Caldas, Colombia. His research interests include mathematical optimization, power systems planning and control, renewable energies, energy storage, protective devices, passivity-based control, and dynamical analysis.

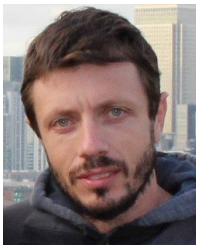

FEDERICO MARTIN SERRA was born in Villa Mercedes, Argentina, in 1981. He received the Electrical and Electronics Engineering degree from Universidad Nacional de San Luis, Argentina, in 2007, and the Ph.D. degree in engineering sciences from Universidad Nacional de Río Cuarto, Argentina, in 2013. Since 2012, he has been the Director of Laboratorio de Control Automático (LCA), Universidad Nacional de San Luis. He is currently the Vice-Dean and a Professor with the Engineering and Agricultural Sciences Department, Universidad Nacional de San Luis, and an Adjunct Researcher with Consejo Nacional de Investigaciones Científicas y Técnicas (CONICET). His research interests include the modeling and advanced control of power converters in applications involving microgrids, electric vehicles, and renewable energy conversion systems.

WALTER GIL-GONZÁLEZ (Senior Member, IEEE) was born in Pereira, Colombia, in 1986. He received the B.Sc., M.Sc., and Ph.D. degrees in electrical engineering from Universidad Tecnológica de Pereira, Colombia, in 2011, 2013, and 2019, respectively, and the Ph.D. degree in renewable energy from the University of Jaén, Spain, in 2024. He previously was an Adjunct Professor with Institucion Universitaria Pascual Bravo. He is currently a Professor with Universidad Tecnológica de Pereira. His research interests include power systems control, stability, optimization, and operation.

LUIS FERNANDO GRISALES-NOREÑA (Member, IEEE) received the master's degree in electrical engineering from Universidad Tecnológica de Pereira, Colombia, in 2015, and the Ph.D. degree in automatic engineering from Universidad Nacional de Colombia, in 2020. He was an Electrical Engineer, in 2013. He has been a University Professor of electrical engineering for more than eight years, with four years of experience in the industry as both engineer and researcher. Moreover, he led a research seedbed for six years. His area of expertise deals with the modeling, planning, and smart operation of electrical networks while considering distributed energy resources (smart grids) in both alternating and direct current systems.

JESÚS C. HERNÁNDEZ (Senior Member, IEEE) was born in Jaén, Spain. He received the M.Sc. and Ph.D. degrees from the University of Jaén, in 1994 and 2003, respectively. Since 2023, he has been a Full Professor with the Department of Electrical Engineering, University of Jaén. His current research interests include smart grids, smart meters, renewable energy, and power electronics.